Topic:

Simulating Molecule Immobilization and Electrochemical Impedance Spectroscopy on a Microfluidic Aptasensor

I. Background description

• Introduction

The rapid, sensitive, real-time and selective detection of tumor markers are becoming more critical due to the arising demand of early diagnostics and point-of-care applications. Aptamers are artificially synthesized DNA or RNA that are selected *in vitro* using Systematic Evolution of Ligands by Exponential Enrichment (SELEX)[1]. They can be specifically evolved to attain great affinity and selectivity against tumor markers such as MUC1[2]. Due to the low immunogenicity and toxicity compared with antibodies[3], aptamer-based sensors (aptasensors) have attracted wide attention and are being more intensively studied during the past few years[4].

Among the variety of biosensing detection methods, electrochemical impedance spectroscopy (EIS) serves as a commonly used one regarding its ability for monitoring different stages during the fabrication process of aptasensors. EIS measures the current and its phase of an electrochemical system when giving oscillating voltages[5]. Upon binding of the analyte to the electrode surface, interfacial electron transfer kinetics gives rise to the change of the impedance measured at different oscillation frequencies. Moreover, the label-free, simple and highly sensitive features further strengthens its potential of integrating with other applications[6].

Microfluidics are recently recognized as an advantageous technique to perform bioanalysis. Not only can they lower the amount of usage during reactions, but also have the potential to meet real-time, portable, large-scale and high-throughput requirements[7].

• Literature review

The effect of certain parameters(e.g. electrode potential, thermodynamic conditions, pH value, ionic strength) on thiolated DNA probe self-assembled-monolayer(SAM) formation on a gold electrode surface were characterized[8]. In **Figure 1**, a +0.3V potential applied to the working electrode results in a higher initial adsorption rate compared with an open circuit. Moreover, it is clear that the rate of adsorption of DNA probes is consistently faster in high ionic strength solution. Probe immobilization involves an interplay of forces including the short-range chemical interactions of the covalent gold/thiol attachment and the long-range electrostatic repulsion between DNA strands.

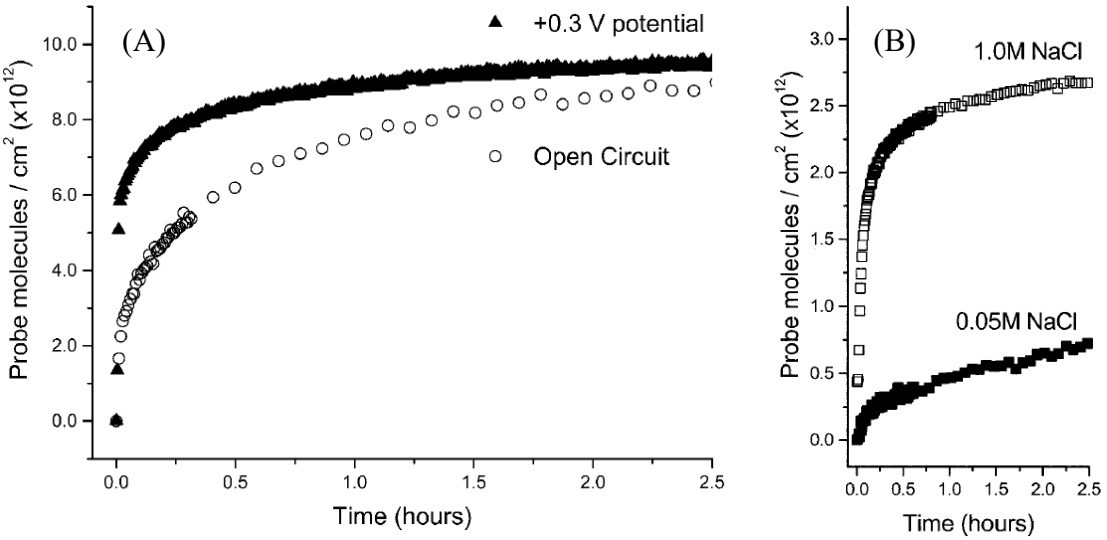

Figure 1. The effect of certain parameters on DNA hybridization. (A) potential-assisted immobilization of probe molecules. (B) comparison of probe immobilization kinetics as a function of ionic strength formed from solutions. [8]

Xi Liu et al fabricated a simple and sensitive impedimetric aptasensor for the detection of tumor markers based on gold nanoparticles signal amplification[9]. The Electrochemical impedance spectra of the measurements performed by EIS during the fabrication process of the aptasensor is shown in **Figure 2**.

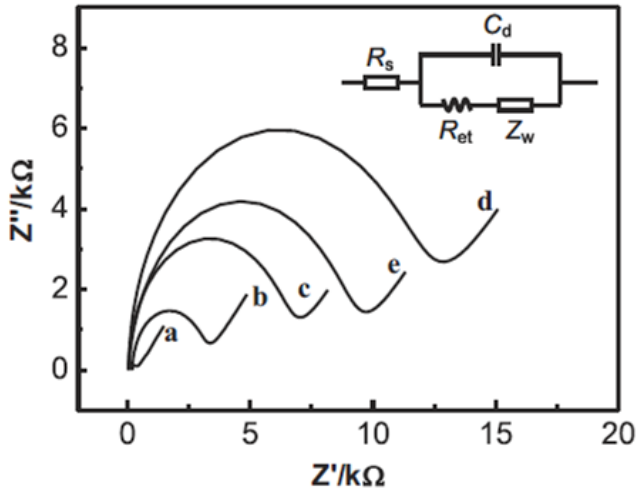

Figure 2. Electrochemical impedance spectra (Nyquist plots) of (a) the bare Au electrode, (b) the Au/cDNA electrode, (c) the Au/cDNA/MCH electrode, (d) the Au/cDNA/MCH/Apt@AuNPs electrode, (e) the Au/cDNA/MCH/Apt electrode

The impedance magnitude generally increases at every stage. **Scheme 1** illustrates a typical fabrication and detection process of an impedimetric aptasensor for detecting the tumor marker MUC1.

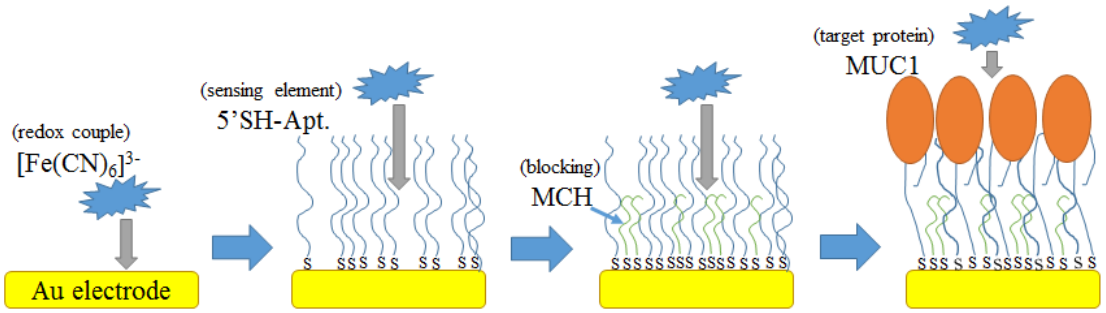

Scheme 1. Fabrication and detection mechanism of an aptasensor. $[Fe(CN)_6]^{3-}$ is used as the redox couple. Firstly, thiolated MUC1 aptamers are immobilized on the Au electrode surface, followed by blocking of Mercaptohexanol(MCH). Detection of MUC1 is further performed.

The behavior of faradic and non-faradic charge transfer reactions can be modeled using an equivalent circuit from the preceding Nyquist plot. **Figure 3** shows a typical Randles circuit[10]. Within each stage of EIS measurement, the Charge transfer resistance(R_{ct}) and Double layer capacitance(C_{dl}) depends largely on surface property.

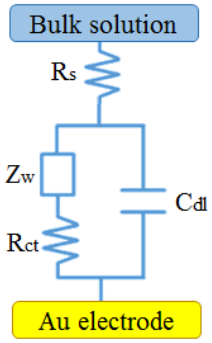

Figure 3. Randles circuit schematic coupled with a gold electrode and bulk solution

• Problem statement

The microfluidic impedimetric aptasensor capable of detecting a certain tumor marker possesses a large potential for real-time and portable developments that even can be applied for integrating with a smart phone's application.

Even so, the long duration of chip fabrication due to micro-processing (e.g. PR, soft lithography, physical vapor deposition), expensive instrument setup usage (e.g. Electrochemical impedance analyzer, syringe pump) and complicated materials and methods (e.g. preparation of buffers, aptamers, proteins) are still to be questioned: Would the aptasensor really be a cost effective method of tumor marker detection?

II. Methods

- **Fabrication process**

An aluminum mold of the PDMS microfluidic channel is priorly fabricated using a CNC machine. **Figure 4** illustrates the remaining processes of the aptasensor fabrication. **Figure 5** specifies the detailed dimensions of the aptasensor. **Figure 6** is a photograph of the sensing region under an optical microscope

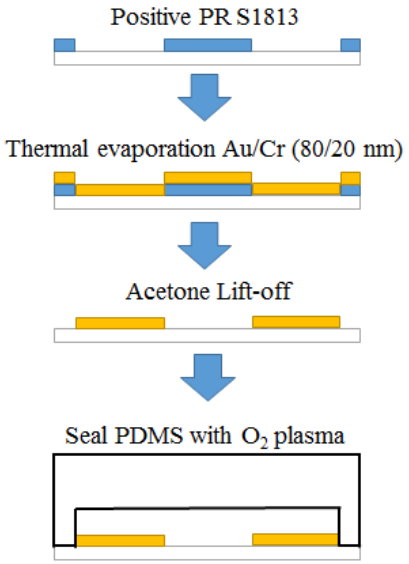

Figure 4. Fabrication process of the Microfluidic Aptasensor

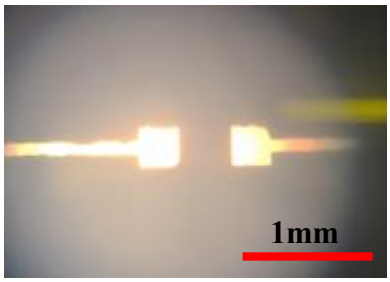

Figure 6. A photograph of the sensing region under an optical microscope

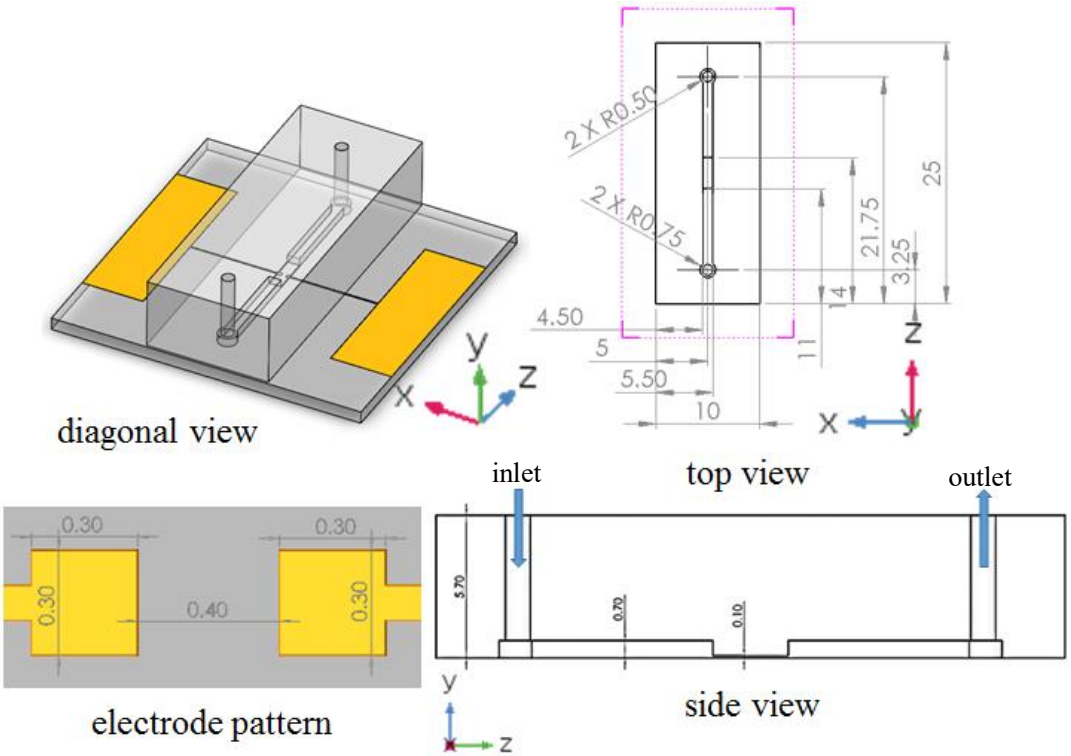

Figure 5. Detailed dimension of the aptasensor

- **Proposed methods and experimental setup**

There are 3 main experimental methods in this study:

1. Feasibility of dimension reduction modeling

Complete 3D simulation approximates real situation the most with no doubt. Nevertheless, the large amount of calculation often takes a lot of time. So we check the feasibility of dimension reduction simulating by performing a stationary 3D laminar flow simulation inside the microfluidic channel, further slicing the 2D planes along a certain direction (zy plane for immobilization simulation and xy plane for EIS simulation) and analyzing the variation of velocity.

2. Molecule immobilization simulation

Different concentrations of molecules are simulated to flow through the microfluidic channel and immobilization rates are compared.

3. EIS simulation

Arbitrarily defined C_{dl} and R_{ct} are set as parameters and the corresponding Electrochemical impedance spectra are compared.

- **Preliminary data**

※All of the animated gif files are included in the supplementary data folder

1. Feasibility of dimension reduction modeling

Physics : Laminar Flow

Navier-Stokes equation:

$$\underbrace{\rho(\mathbf{u}\cdot\nabla)\mathbf{u}}_{\text{Inertia}} = \nabla\cdot\underbrace{[-pI}_{\text{Pressure}} + \underbrace{\mu(\nabla\mathbf{u}+(\nabla\mathbf{u})^{\mathrm{T}}]}_{\text{Viscous}} + \mathrm{F}$$

Study : Stationary

$$\rho\nabla\cdot\mathbf{u} = 0$$

Fluid : Water

P_{inlet} = 1Pa

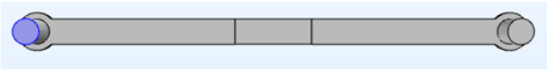

P_{outlet} = 0Pa

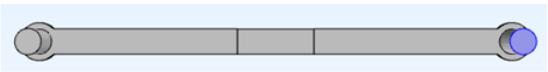

Mesh Size : Normal

Velocity profiles are sliced at the zy and xy plane and are depicted in **Figure 6** with arbitrary x and z positions. On the xy plane in **Figure 6** (A), the variation of velocity at different z positions are very low by naked eye observation. But on the zy plane, the velocity decreases sharply at sliced plane near the channel side. This is due to the laminar no-slip effect. **Figure 7** shows the velocity profile at y = 0.05mm. Velocity changes sharply at approximately 0 – 0.25mm (x = 0.25 – 0.50mm) from the channel side. Velocity magnitude are further plotted at 5 different z positions in **Figure 8** (z = 9.70, z = 9.85, z = 10.00, z = 10.15, z = 10.30 mm). At x = 0.5 – 1.0mm the velocity is

approximately 3.3mm/s. These results demonstrate that dimension reduction simulation on the xy plane is feasible at around z = 9 – 11mm and is feasible on the zy plane at x = 0.5 – 1.0mm.

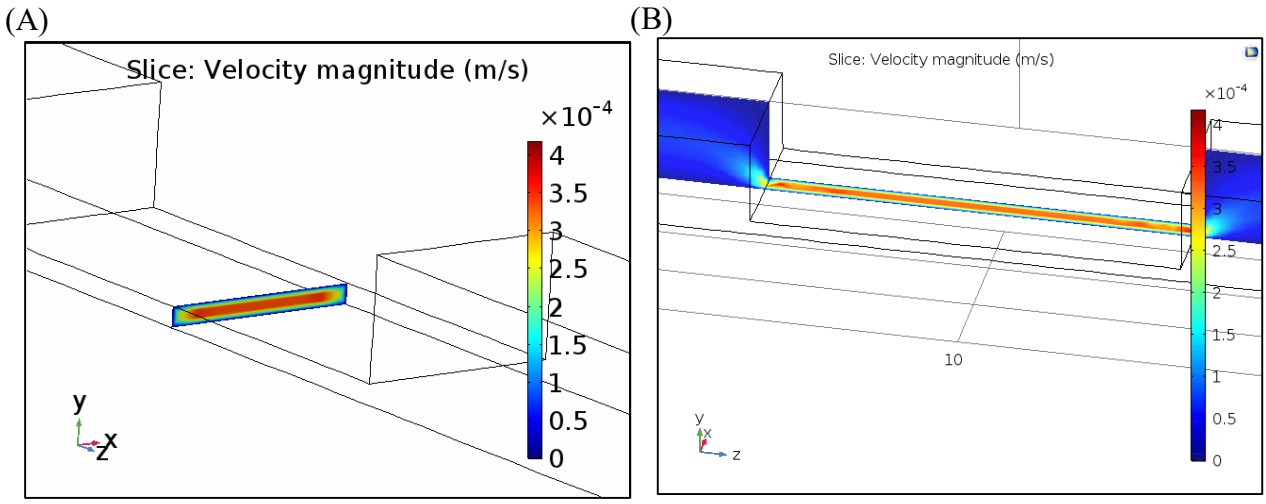

Figure 6. Velocity profiles on sliced planes. (A) On the xy plane. (B) On the zy plane.

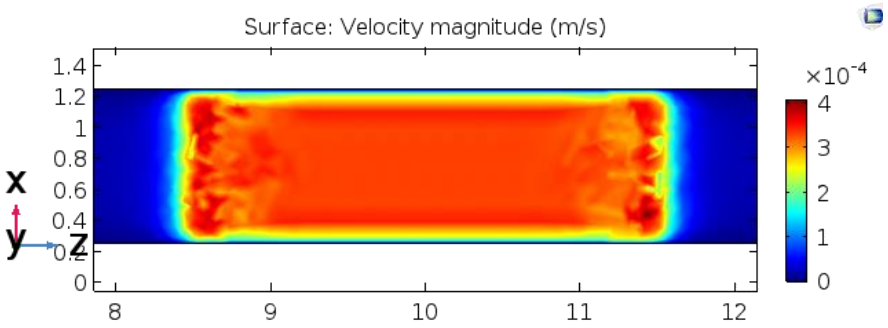

Figure 7. Velocity profile at y = 0.05mm

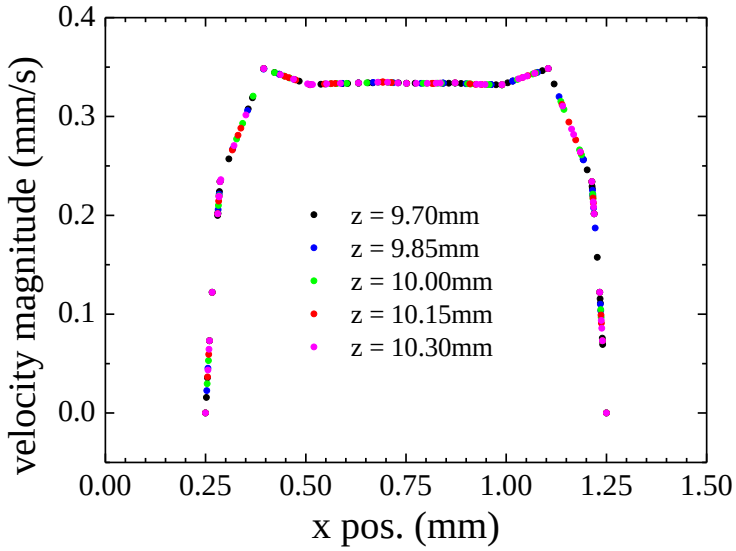

Figure 8. Velocity magnitude at y = 0.05mm

2. Molecule immobilization simulation

Physics : i. Transport of Diluted Species
ii. General Form Boundary PDE

Convection–diffusion equation :

$$\frac{\partial c}{\partial t} + \underbrace{\nabla \cdot (-D\nabla c)}_{\text{diffusion}} + \underbrace{\mathbf{u} \cdot \nabla c}_{\text{convection}} = \overbrace{R}^{\text{inlet \& outlet}}$$

conc. flux $\mathbf{N} = -D\nabla c + \mathbf{u}c$

Transport and Adsorption equation :

$$\frac{\partial c_s}{\partial t} + \underbrace{\nabla \cdot (-D\nabla c_s)}_{\text{surface diffusion}} = \underbrace{k_{ads} c(\Gamma_s - c_s) - k_{des} c_s}_{\text{Langmuir Adsorption Isotherm}}$$

Study : Time dependant

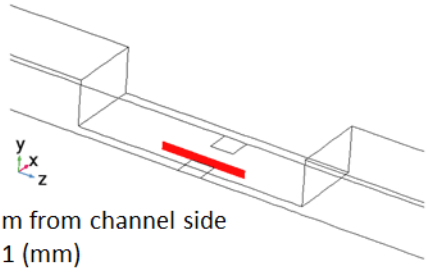

x = 0.3mm from channel side
y = 0 - 0.1 (mm)
z = 9.45 - 10.55 (mm)

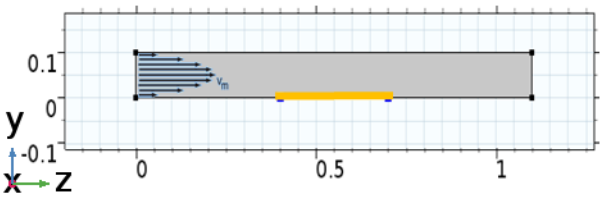

Table 1. Molecule immobilization simulation parameters

Parameter	Value	Description
D	10^{-9} m²/s	molecule diffusivity
D_s	0.35 mm/s	surface diffusivity
Γ_s	$1.6\text{x}10^{-7}$ mol/m²	maximum molecule density
k_{des}	10^{-20} 1/s	desorption constant
k_{ads}	$1.9\text{x}10^{3}$ 1/(M×s)	adsorption constant
c_0	0.1 ~ 10 μM	inlet concentration
v_{max}	0.35 1/(mm×s)	maximum velocity

Adsorption of molecules are simulated within a 2D dimensional channel. The reaction is modeled by transport of diluted species of the molecule and the Langmuir adsorption isotherm (general form boundary PDE). Fully developed laminar flow between two parallel plates characterized the fluid velocity profile. It is clear that in **Figure 9**, a higher concentration of inflow molecule results in a faster adsorption rate. At concentrations above 0.1μM, the probe density almost saturates to a value of $9.6\text{x}10^{12}$ molecules/cm^2 before immobilizing for 10 hours. The result highly resembles a typical binding curve, suggesting the possibility for computer simulating assisted optimization of *in vitro* parameters.

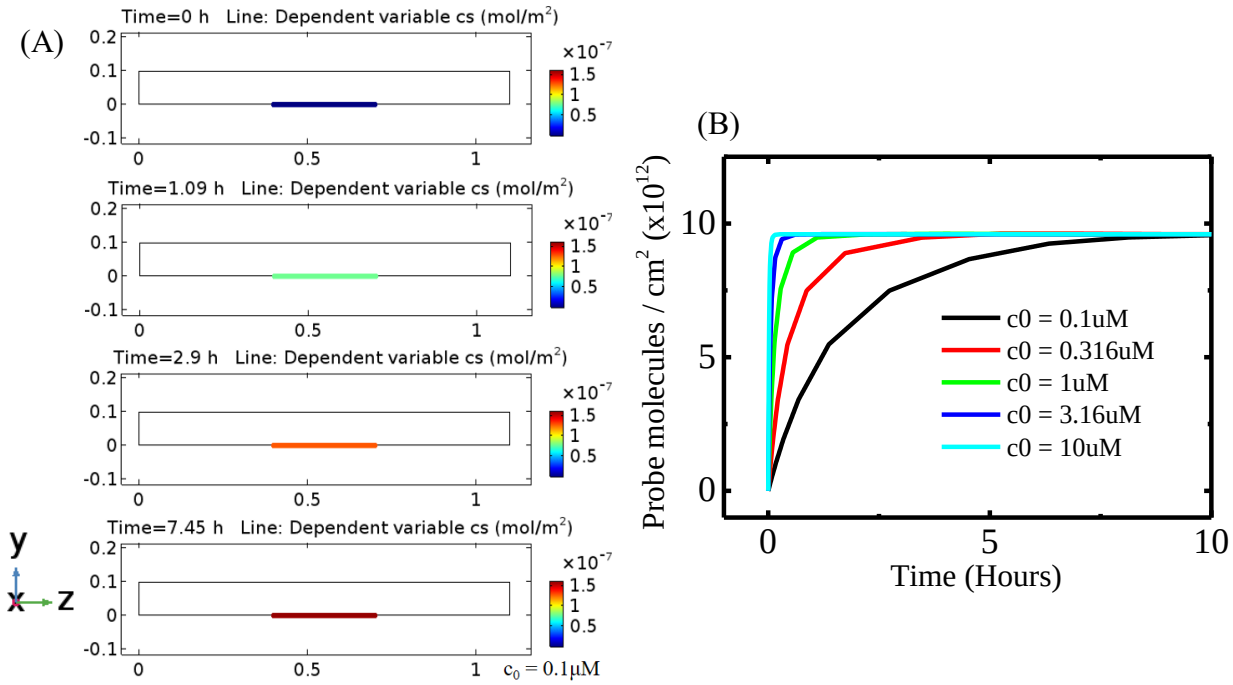

Figure 9. Time dependent surface probe density variation. (A) The probe density on the simulated gold electrode (z = 0.4 – 0.7mm). The inflow molecule concentration is c_0 = 0.1μM. (B) Time dependent molecule immobilization plot at z = 0.55mm.

3. EIS simulation

Physics : Electroanalysis

Fick's 2nd law (diffusion equation) :

$$\frac{\partial c}{\partial t} = \nabla \cdot (D \nabla c)$$

Butler-Volmer equation :

$$j = nFk_0(c_{Red}e^{\frac{(n-\alpha_c)F\eta}{RT}} - c_{Ox}e^{\frac{-\alpha_c F\eta}{RT}})$$

Current density

Study :

- Parametric Sweep
- Frequency-Domain Perturbation

Mesh : Extremely fine

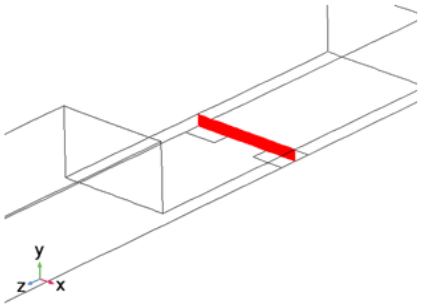

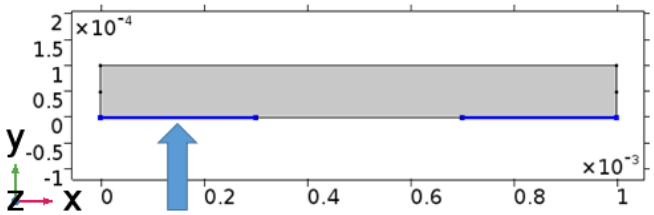

working electrode (WE)

Table 2. EIS simulation parameters

Parameter	Value	Description
n	1	number of electrons
k_0	$10^{-3} \sim 10^{-1}$ cm/s	heterogeneous rate constant
η	0 V	overpotential ($E - E_{eq}$)
c_{Red}	1 mol/m³	reductant concentration
c_{Ox}	1 mol/m³	oxidant concentration
α_c	0.5	cathode transfer coefficient
C_{dl}/A	$10^{-2} \sim 10^{2}$ μF/cm²	double layer capacitance/area

The charge transfer resistance (R_{ct}) is related to the surface diffusivity by:

$$R_{ct} = \frac{RT}{n^2F^2Ak_0({c_{Ox}}^{\alpha_c})({c_{Red}}^{n-\alpha_c})}$$

where R is the universal gas constant, T is the temperature, F is the faraday constant, A is the area of the electrode and c is the bulk concentration of redox couple (in this case $c_{Red} = c_{Ox} = 1$ mol/m³).

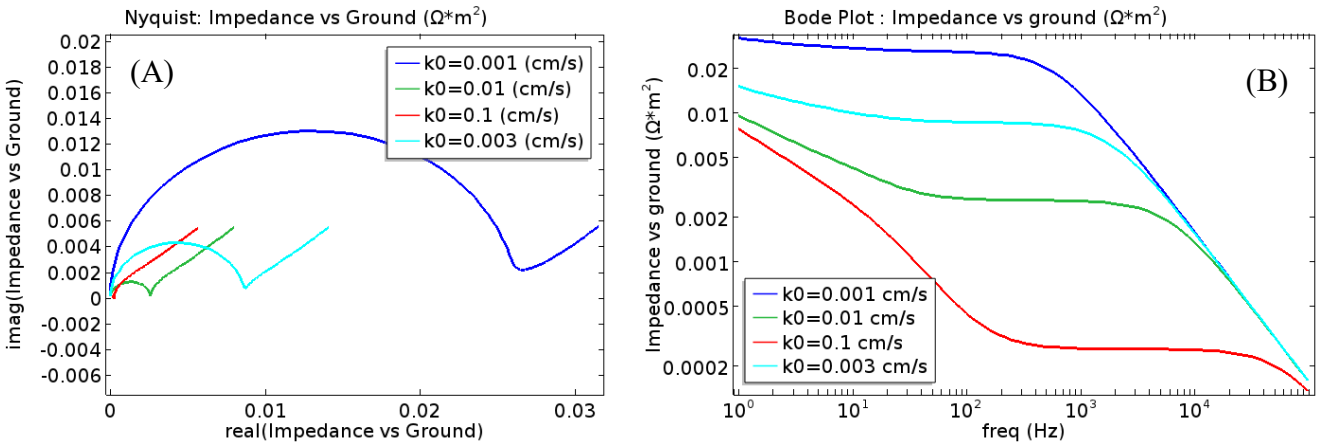

Figure 10. Simulated electrochemical impedance spectra with capacitance density C_{dl}/A = 1μF/cm². (A) Nyquist plot. (B) Bode plot.

The heterogeneous rate constant (k_0) directly defines the charge transfer resistance (R_{ct}) in the Randles equivalent circuit model (**Figure 3**). We can see from the Nyquist plot (**Figure 10** (A)) that the semicircle gets bigger due to smaller k_0, or correspondingly, a larger R_{ct}. In the Bode plot (**Figure 10** (B)), smaller k_0 results in a generally larger impedance at low frequencies but still converges to a single point as the frequency gets higher and higher. **Figure 2** resembles **Figure 10** (A) comparing the size variation of the semicircles, suggesting that the immobilization of aptamers, blocking and protein immobilization lowers k_0 in every stage.

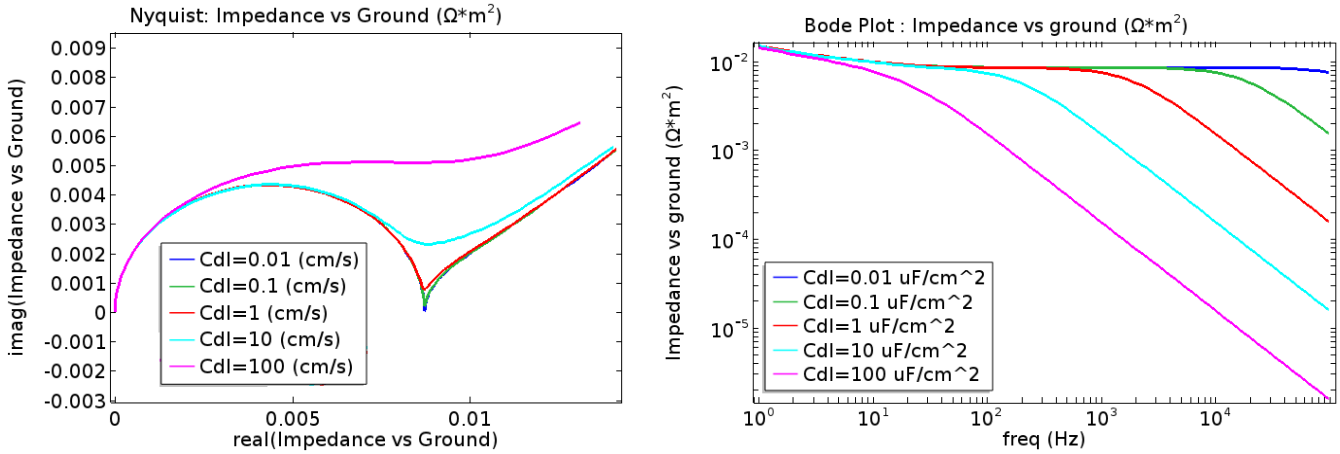

Figure 11. Simulated electrochemical impedance spectra with heterogeneous rate constant $k_0 = 3\times10^{-3}$cm/s. (A) Nyquist plot. (B) Bode plot.

In **Figure 11** (A), a larger double layer capacitance (C_{dl}) results in a smoother transformation of the semicircle curve to the 45° straight line which originates from diffusion dominated transport of the electrolyte[11], but does not have an effect on the size of the semicircle. In **Figure 11** (B), the impedance drops at lower frequencies when possessing a larger C_{dl}. This electrokinetic phenomena is due to the fact that the storing of electrical energy within the double layer can compensate to the current flow more at higher frequencies. The above results resemble the electrochemical impedance spectra measured in the fabrication process and detection stage of an impedimetric aptasensor, which also suggests the possibility for computer simulating assisted optimization of *in vitro* parameters.

• Potential problems and solutions

The method and results in the above mentioned simulations all face some realities which can't possibly be modeled or would encounter large difficulties when modeling.

For instance, it would be more difficult to setup the reference electrode (RE) for EIS measurements in a microfluidic channel, which means that only a two electrode electrochemical cell system is installable. The corresponding reaction occurring in EIS measurements would become more complicated to model, resulting in a more complicated equivalent circuit. This problem may be solved by simulating a counter electrode and measuring the impedance difference of the working electrode and the counter electrode.

Another problem is the microscale effect in probe immobilization, such as the repulsion between molecules such as negatively charged DNA aptamers, which might lower the probe density compared with totally neutral molecules. This can be modeled by setting up electrokinetic parameters in the buffer and diluted species and can further attain data due to the variations of ionic strength of the buffer.

III. Conclusions and Future works

In this report, the feasibility of dimension reduction modeling of a microfluidic impedimetric aptasensor on the zy and xy plane was qualitatively studied, permitting further 2D model simulations. Immobilization of different concentrations of thiolated molecules onto a gold electrode surface are simulated. EIS analysis simulation with variating heterogeneous rate constant and double layer capacitance are also performed.

Further wet lab experimental validation of certain parameters and development of more realistic models are to be scheduled and done.

IV. References

1. Ellington, A.D. and J.W. Szostak, *In vitro selection of RNA molecules that bind specific ligands.* Nature, 1990. **346**(6287): p. 818-822.
2. Ferreira, C.S.M., C.S. Matthews, and S. Missailidis, *DNA Aptamers That Bind to MUC1 Tumour Marker: Design and Characterization of MUC1-Binding Single-Stranded DNA Aptamers.* Tumor Biology, 2006. **27**(6): p. 289-301.
3. Brody, E.N. and L. Gold, *Aptamers as therapeutic and diagnostic agents.* Reviews in Molecular Biotechnology, 2000. **74**(1): p. 5-13.
4. Shieh, Y.-A., et al., *Aptamer-Based Tumor-Targeted Drug Delivery for Photodynamic Therapy.* ACS Nano, 2010. **4**(3): p. 1433-1442.
5. Katz, E. and I. Willner, *Probing Biomolecular Interactions at Conductive and Semiconductive Surfaces by Impedance Spectroscopy: Routes to Impedimetric Immunosensors, DNA-Sensors, and Enzyme Biosensors.* Electroanalysis, 2003. **15**(11): p. 913-947.
6. Macdonald, J.R. and E. Barsoukov, *Impedance spectroscopy: theory, experiment, and applications.* History, 2005. **1**(8).
7. Liu, Y., et al., *Multilayer-Assembled Microchip for Enzyme Immobilization as Reactor Toward Low-Level Protein Identification.* Analytical Chemistry, 2006. **78**(3): p. 801-808.
8. Peterson, A.W., R.J. Heaton, and R.M. Georgiadis, *The effect of surface probe density on DNA hybridization.* Nucleic Acids Research, 2001. **29**(24): p. 5163-5168.
9. Liu, X., et al., *A simple and sensitive impedimetric aptasensor for the detection of tumor markers based on gold nanoparticles signal amplification.* Talanta, 2015. **132**: p. 150-154.
10. Randles, J.E.B., *Kinetics of rapid electrode reactions.* Discussions of the Faraday Society, 1947. **1**(0): p. 11-19.
11. Bard, A. and L. Faulkner, *Electrochemical Methods: Fundamentals and Applications*. 2001: John Wiley & Sons, Inc.